Large-scale latitudinal and vertical distributions of NMHCs and selected halocarbons in the troposphere over the Pacific Ocean during the March-April 1999 Pacific Exploratory Mission (PEM-Tropics B)

Nicola J. Blake[1], Donald R. Blake[1], Isobel J. Simpson[1], Jimena P. Lopez[1], Nancy A. C. Johnston[1], Aaron L. Swanson[1], Aaron S. Katzenstein[1], Simone Meinardi[1], Barkley C. Sive[1, 2], Jonah J. Colman[1], Elliot Atlas[3], Frank Flocke[3], Stephanie A. Vay[4], Melody A. Avery[4], and F. Sherwood Rowland[1]

Abstract. Nonmethane hydrocarbons (NMHCs) and selected halocarbons were measured in whole air samples collected over the remote Pacific Ocean during NASA's Global Tropospheric Experiment (GTE) Pacific Exploratory Mission-Tropics B (PEM-Tropics B) in March and early April 1999. The large-scale spatial distributions of NMHCs and C_2Cl_4 reveal a much more pronounced north-south interhemispheric gradient, with higher concentrations in the north and lower levels in the south, than for the late August to early October 1996 PEM-Tropics A experiment. Strong continental outflow and winter-long accumulation of pollutants led to seasonally high Northern Hemisphere trace gas levels during PEM-Tropics B. Observations of enhanced levels of Halon 1211 (from developing Asian nations such as the PRC) and CH_3Cl (from SE Asian biomass burning) support a significant southern Asian influence at altitudes above 1 km and north of 10°N. By contrast, at low altitude over the North Pacific the dominance of urban/industrial tracers, combined with low levels of Halon 1211 and CH_3Cl, indicate a greater influence from developed nations such as Japan, Europe, and North America. Penetration of air exhibiting aged northern hemisphere characteristics was frequently observed at low altitudes over the equatorial central and western Pacific south to ~5°S. The relative lack of southern hemisphere biomass burning sources and the westerly position of the South Pacific convergence zone contributed to significantly lower PEM-Tropics B mixing ratios of the NMHCs and CH_3Cl south of 10°S compared to PEM-Tropics A. Therefore the trace gas composition of the South Pacific troposphere was considerably more representative of minimally polluted tropospheric conditions during PEM-Tropics B.

1. Introduction

Nonmethane hydrocarbons (NMHCs) have diverse natural and anthropogenic emission sources and relatively short atmospheric lifetimes, ranging from months to hours. The main sink of NMHC or halocarbon gases with an extractable hydrogen atom, or with an unsaturated bond, is through reaction with OH radicals. The oxidation of NMHCs can lead to the formation of tropospheric O_3 via a combination of sunlight together with sufficient concentrations of nitrogen oxides (NO_x) [*Crutzen*, 1973].

Trace gas distributions provide information crucial to establishing the extent of continental influence on the chemical environment of the remote troposphere. The average atmospheric lifetimes of ethane, ethyne, and C_2Cl_4 are much less than the 1-year average interhemispheric exchange time. However, they are comparable to mixing times within a hemisphere (~ 2-6 weeks depending on latitude and season [*Seinfeld and Pandis*, 1998]). Therefore the NMHCs and C_2Cl_4 show significant latitudinal, seasonal, and vertical gradients in the atmosphere [*Blake and Rowland*, 1986; *Singh et al.*, 1988; *Wang et al.*, 1995]. Sharp latitude gradients in CO and ethane, with higher mixing ratios in the Northern Hemisphere, were observed at all altitudes near the intertropical convergence zone (ITCZ) by *Blake et al.* [1997], and at high altitude by *Matsueda et al.* [1998]. CO and other short-lived species (NMHCs, C_2Cl_4, etc.) have been employed to study the dynamical structure of the ITCZ and South Pacific convergence zone (SPCZ) regions [e.g., *Gregory et al.*, 1999].

Several research groups have monitored the seasonal accumulation of NMHCs at the surface and at low altitudes (<3 km) in the Northern Hemisphere [e.g., *Singh and Salas*, 1982; *Blake and Rowland*, 1986; *Penkett et al.*, 1993;

---

[1]Department of Chemistry, University of California, Irvine, California.

[2] Now at Department of Chemistry, Central Michigan University, Mt. Pleasant, Michigan.

[3] Atmospheric Chemistry Division, National Center for Atmospheric Research, Boulder, Colorado.

[4] NASA Langley Research Center, Atmospheric Sciences Division, Hampton, Virginia.

Greenberg et al., 1996]. However, the latitudinal and seasonal variations of NMHCs in the Southern Hemisphere are poorly known [*Blake and Rowland*, 1986; *Rudolph et al.*, 1989, 1992], especially for higher molecular weight (>C_3) compounds [*Bonsang and Boissard*, 1999].

Until recently, few NMHC and halocarbon measurements had been made in the troposphere over the Pacific. *Ridley et al.* [1997] conducted aircraft measurements of NMHCs near Hawaii. However, most other NMHC measurements in the Pacific region have been made during limited shipboard studies [e.g., *Atlas et al.*, 1993; *Donahue and Prinn*, 1993]. Our observations for the NASA GTE Pacific Exploratory Mission (PEM) West A and PEM West B projects are among the most comprehensive available. They describe the large-scale tropospheric distribution over the northwestern Pacific region during both the Northern Hemisphere summer and winter seasons [*Blake, D. R. et al.*, 1996; *Blake et al.*, 1997]. More recently, in August-September 1996, PEM-Tropics A provided the first detailed survey of tropospheric chemistry, including the vertical and spatial distributions of NMHCs and halocarbons over the South Pacific Basin [*Hoell et al.*, 1999; *Blake et al.*, 1999a]. A latitudinal survey of the Pacific Ocean was conducted during the first Aerosol Characterization Experiment (ACE-1) in November 1995 [*Blake et al.*, 1999b]. Both PEM-Tropics A and ACE-1 revealed significant influence from biomass burning emissions over the remote South Pacific during the southern-tropical dry season. Air trajectory analyses point strongly toward these emissions as having been transported from South America, Africa, and Oceania.

The PEM-Tropics B field campaign took place in the southern-tropical wet season, when the influence from biomass burning was predicted to be minimal. It therefore provided a different seasonal perspective on the tropospheric chemistry of the tropical Pacific [*Raper et al.*, this issue]. This paper focuses on results from the nonmethane hydrocarbon and halocarbon analysis of samples collected aboard the DC-8 and P-3B aircraft during PEM-Tropics B.

2. Experiment

We filled our 2-L stainless steel sampling canisters with whole air from beyond the laminar boundary layer of the aircraft and pressurized to 40 psi employing a two-stage metal bellows pump (Parker MB-602XP). Approximately 140 samples were collected during a typical 8-hour DC-8 flight, and 120 canisters for each 8-hour flight aboard the P-3B. These samples were obtained roughly every 3-7 min during horizontal flight legs and 1-3 min during vertical legs. The P-3B typically flew at low levels (0.1-7.5 km) whereas the DC-8 operated at higher altitudes (5-12 km) with occasional excursions into the boundary layer. During both horizontal and vertical flight legs our sampling duration was a minimum of 8 s at low altitude (150 m) to ~ 80 s at high altitude (11 km). Sampling time during horizontal legs was usually adjusted to be ~ 1 min, corresponding to an approximate sampling distance of 8-12 km. Typical vertical sampling distances were 300 m for the DC-8, and 150 m for the P-3B.

After each flight, the filled canisters were transported to our laboratory at the University of California-Irvine (UCI) via courier for analysis within 10 days. Each sample was analyzed for more than 50 trace gases comprising hydrocarbons, halocarbons, and alkyl nitrates [*Sive*, 1998; also Sive et al., manuscript in preparation, 2001]. In addition, we recently expanded our analytical capabilities to include DMS measurements [*Simpson et al.*, 2000]. Two identical analytical systems sharing the same standards were operated simultaneously around the clock to improve canister turnaround time and to keep our measurement precision optimal.

One thousand five hundred twenty ± 1 cm^3 (STP) of air was preconcentrated on glass beads in a liquid nitrogen-cooled stainless steel loop, warmed, then helium carrier gas flushed the contents of the loop to a splitter (Valco Instruments, 1/16" manifold 1 to 6 ports, 0.75-mm inlet bore, 0.25-mm outlet bore, with one outlet port capped off). Here the sample was split and directed to five different gas chromatographic columns via Silcosteel tubing (0.28 mm I.D., Restek Corporation). With the exception of the megabore PLOT column (see later), which had a 2.5-cm-long piece of 0.1-mm I.D. fused silica tubing installed to restrict the flow, the relative sample amount passing through an individual column was dependent primarily on the column inner diameter. As long as the specific humidity of the injected air was above a certain level, the split ratio was always highly reproducible during PEM-Tropics B. We ensured sufficient sample humidity by adding 1.3 kPa of water to each evacuated canister just before it was sent out to the field. We monitored the split ratio by comparing the calculated mixing ratios for selected compounds that give large signals, have good chromatographic characteristics, and are quantified on multiple detectors, typically CFC-11 and propane.

The unique separation and detection characteristics of each of the five column-detector combinations employed during PEM-Tropics B were optimal for a particular subset of NMHC or halocarbon gases, and in combination provided a comprehensive suite of trace gas measurements. The first column-detector combination (abbreviated as "DB5ms/MSD") was a DB-5ms column (J&W; 60 m, 0.25 mm I.D., 0.5-µm film thickness) output to a quadrapole mass spectrometer detector (MSD) (HP-5973). The second combination ("DB1/FID") was a DB-1 column (J&W; 60 m, 0.32 mm I.D., 1-µm film thickness) output to a flame ionization detector (FID) (HP-6890). The third combination ("PLOT-DB1/FID") was a PLOT column (J&W GS-Alumina; 30 m, 0.53 mm I.D.) connected in series to a DB-1 column (J&W; 5 m, 0.53 mm I.D., 1.5-µm film thickness) and output to an FID. The fourth combination ("Restek1701/ECD") was a RESTEK 1701 column (60 m, 0.25 mm I.D., 0.50-µm film thickness), which was output to an ECD. The fifth combination ("DB5-Restek1701/ECD") was a DB-5 (J&W; 30 m, 0.25 mm I.D., 1-µm film thickness) column connected in series to a RESTEK 1701 column (5 m, 0.25 mm I.D., 0.5-µm film thickness) and output to an ECD. The DB5ms/MS, DB1/FID, PLOT-DB1/FID, Restek1701/ECD, and DB5-Restek1701/ECD combinations received 10.1, 15.1, 60.8, 7.2, and 6.8% of the sample flow, respectively.

Retention times were determined by running qualitative standards spiked into clean (upper tropospheric) air to simulate whole air samples. Detector response factors were also determined by the analysis of synthetic standards spiked into clean whole air. The per carbon response was uniform for gases eluting prior to n-pentane on the PLOT column,
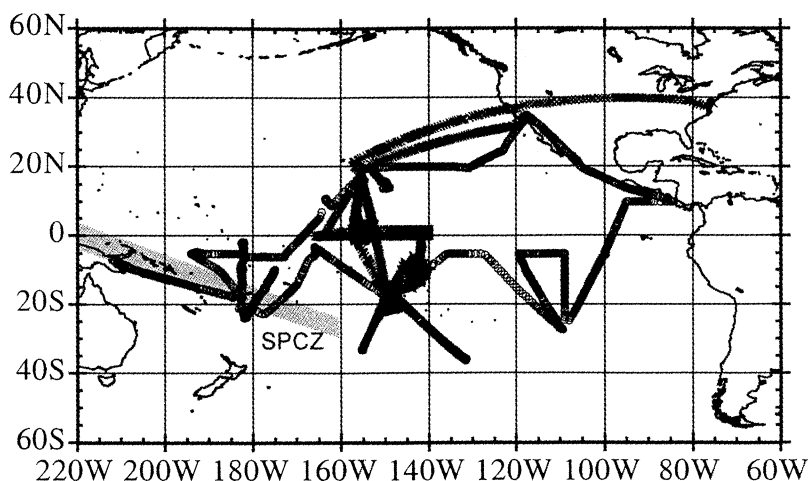
Figure 1. Location of whole-air samples collected at all altitudes aboard the NASA Dryden DC-8 (circles) and the NASA Wallops P-3B (crosses) during PEM-Tropics B. The approximate location of the SPCZ (adapted from *Fuelberg et al.*, [this issue]) is also shown.

however, the per carbon response for n-pentane decreased by almost a factor of two. Therefore, wherever possible we avoided employing the PLOT column for quantitative evaluation of gases eluting later than i-pentane. For the DB-1 column the per carbon response systematically decreased by ~ 2-3% for each increasing carbon number greater than C_3.

Our analytical accuracy ranges from 2 to 20%. NMHC calibrations employed a combination of National Bureau of Standards, Scott Specialty Gases (absolute accuracy estimated to be within ± 5%), and UCI-made standards. We diluted the Scott standards to the low pptv mixing ratio range with helium. These synthetic standards were used to confirm the mixing ratios of previously calibrated cylinders containing whole air at high pressure. For example, just before PEM-Tropics B the 4-year-old calibration of one of our long-term high-pressure whole-air working standards agreed with freshly prepared synthetic standards to better than 1% for the light hydrocarbons (C_2-C_5) and to better than 5% for the C_6-C_{10} hydrocarbons.

Our group at UCI has participated in the National Science Foundation sponsored Nonmethane Hydrocarbon Intercomparison Experiment (NOMHICE) overseen by Drs. Jack Calvert and Eric Apel at NCAR [*Apel et al.*, 1994]. Results from NOMHICE demonstrate that our analytical procedures consistently yield accurate identifications of a wide range of unknown hydrocarbons and produce excellent quantitative results [*Apel et al.*, 1994, 1999; *Sive*, 1998; *Sive et al.*, manuscript in preparation, 2001].

The precision of the measurements varies by compound and by mixing ratio. For example, the measurement precision for the NMHCs is 1% or 1.5 pptv (whichever is larger) for the alkanes and alkynes, and 3% or 3 pptv (whichever is larger) for the alkenes [*Sive*, 1998]. The precision for CFC-12 at 550 pptv is ±3 pptv, while that for methyl iodide at 0.05 pptv is ±0.01 pptv. The limit of detection (LOD) is 3 pptv for the NMHCs and 1 pptv for DMS. Although the LOD is different for each halocarbon, the halocarbons that we report are usually present at mixing ratios well above their detection limits.
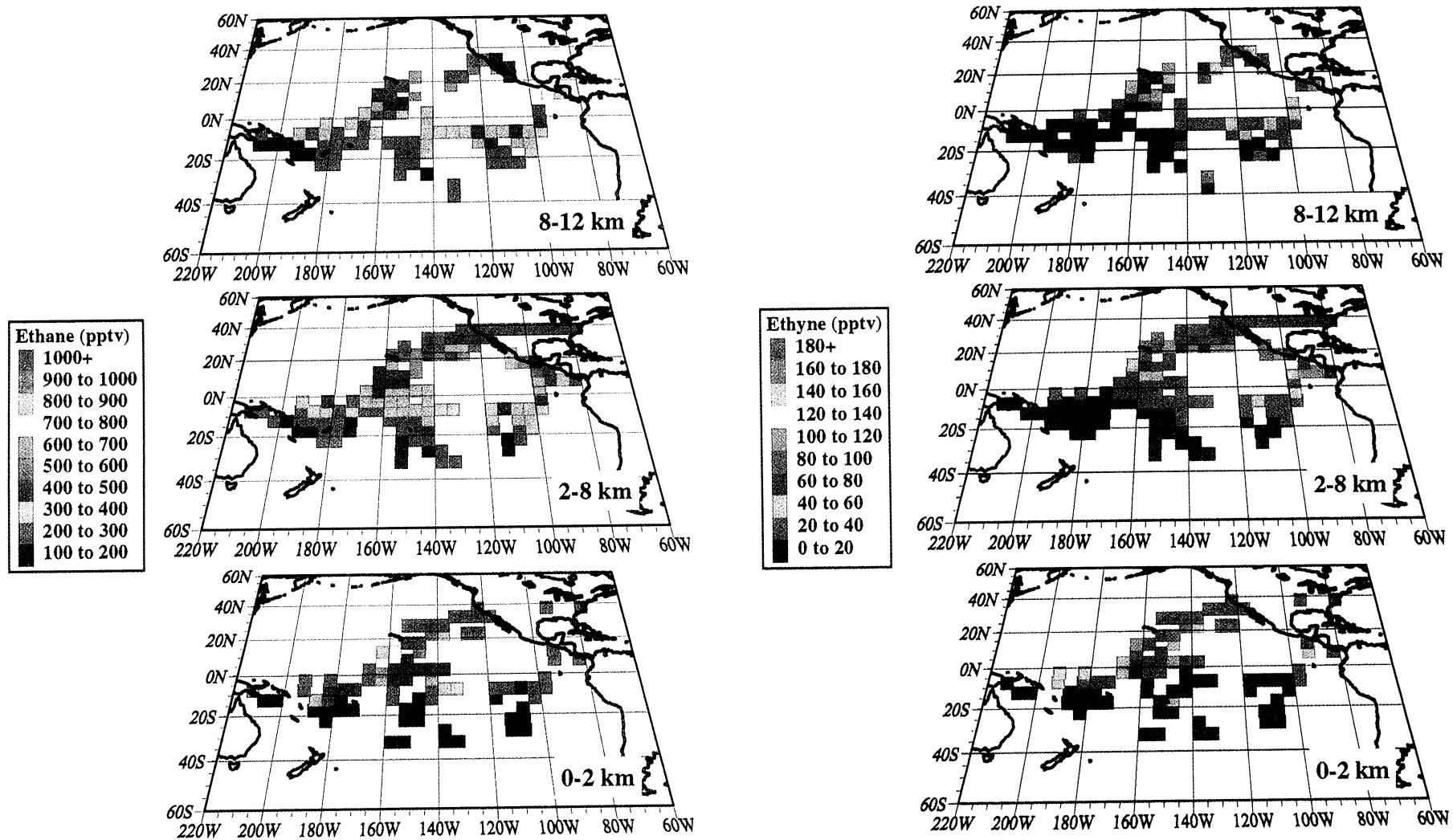
Fast response in situ measurements of CO were made spectroscopically using a folded-path, differential absorption,

tunable diode laser spectrometer during PEM-Tropics A and PEM-Tropics B [*Sachse et al.*, 1991]. In situ O_3 measurements for both PEM-Tropics A and PEM-Tropics B employed NO+O_3 chemiluminescent detectors [*Gregory et al.*, 1987].

The sampling frequencies of the in situ CO and O_3 instruments are much higher than our whole air sampling times. We have employed a merged data file generated at Harvard University and containing CO and O_3 mixing ratios averaged over the whole air sampling times for comparison of the different PEM-Tropics measurement databases. The PEM-Tropics A and PEM-Tropics B measurements and merged data files are archived at NASA Langley Research Center and can be accessed via the GTE web site at http://www-gte.larc.nasa.gov/.

3. Spatial Distribution and Chemical Characteristics

The PEM-Tropics B field campaign was conducted from March to April 1999, with major deployment sites in Hawaii, Kiritimati (Christmas Island), Tahiti, and Fiji [*Raper et al.*, this issue]. Whole-air samples were collected aboard the NASA Dryden DC-8 and the NASA Wallops P-3B research aircraft during the 35 science flights of PEM-Tropics B. Sample locations are displayed on Figure 1. Plate 1 shows 5° by 5° average mixing ratios of these data as latitude-longitude patch plots for ethane, ethyne, C_2Cl_4, CH_3Cl, HCFC-141B, and Halon 1211. These gases were selected to represent a range of lifetimes and source types. For example, incomplete combustion, including urban fossil fuel and biomass burning, is the principal global source of ethane, ethyne, and CO [*Seinfeld and Pandis*, 1998]. As will be shown later, CO serves as a useful gas against which to reference the atmospheric trends of the NMHCs and halocarbons [e.g., *Smyth et al.*, 1996; *Blake, N. J. et al.*, 1996, 1999). NMHCs are also emitted from liquefied petroleum gas leakage, oil drilling and natural gas fields [*Blake and Rowland*, 1995; *Blake et al.*, 1992], C_2Cl_4 is an industrial solvent, CH_3Cl is a product of biomass burning [e.g., *Blake, N. J. et al.*, 1996], HCFC-141B is a CFC substitute whose usage is increasing

Ethane (pptv)
- 1000+
- 900 to 1000
- 800 to 900
- 700 to 800
- 600 to 700
- 500 to 600
- 400 to 500
- 300 to 400
- 200 to 300
- 100 to 200

Ethyne (pptv)
- 180+
- 160 to 180
- 140 to 160
- 120 to 140
- 100 to 120
- 80 to 100
- 60 to 80
- 40 to 60
- 20 to 40
- 0 to 20

Plate 1. Color "patch" plots showing the latitudinal and longitudinal spatial distribution of the mixing ratios of ethane, ethyne, C_2Cl_4, CH_3Cl, HCFC-141B, and Halon 1211 during PEM-Tropics B for three altitude ranges (0-2 km, 2-8 km, and 8-12 km). The data were averaged over 5° by 5° latitude-longitude grids.

C₂Cl₄ (pptv)

■	5.0+
	4.5 to 5.0
	4.0 to 4.5
	3.5 to 4.0
	3.0 to 3.5
	2.5 to 3.0
	2.0 to 2.5
	1.5 to 2.0
	1.0 to 1.5
■	0.5 to 1.0

CH₃Cl (pptv)

■	595+
	585 to 595
	575 to 585
	565 to 575
	555 to 565
	545 to 555
	535 to 545
	525 to 535
	515 to 525
■	505 to 515

Plate 1. (continued)

HCFC-141b (pptv)
- 11.2+
- 10.9 to 11.2
- 10.6 to 10.9
- 10.3 to 10.6
- 10.0 to 10.3
- 9.7 to 10.0
- 9.4 to 9.7
- 9.1 to 9.4
- 8.8 to 9.1
- 8.5 to 8.8

H-1211 (pptv)
- 4.20+
- 4.14 to 4.20
- 4.08 to 4.14
- 4.02 to 4.08
- 3.96 to 4.02
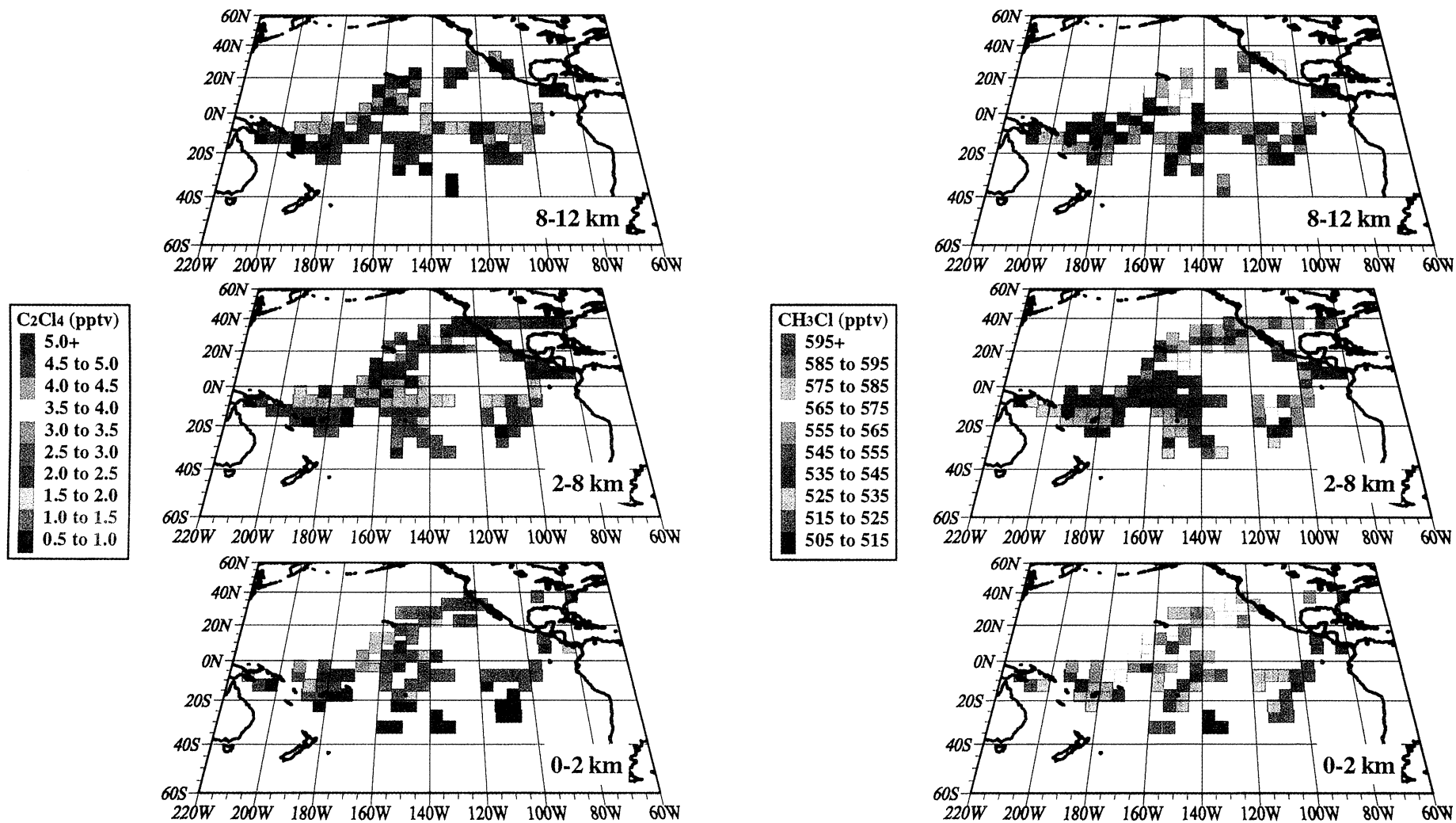- 3.90 to 3.96
- 3.84 to 3.90
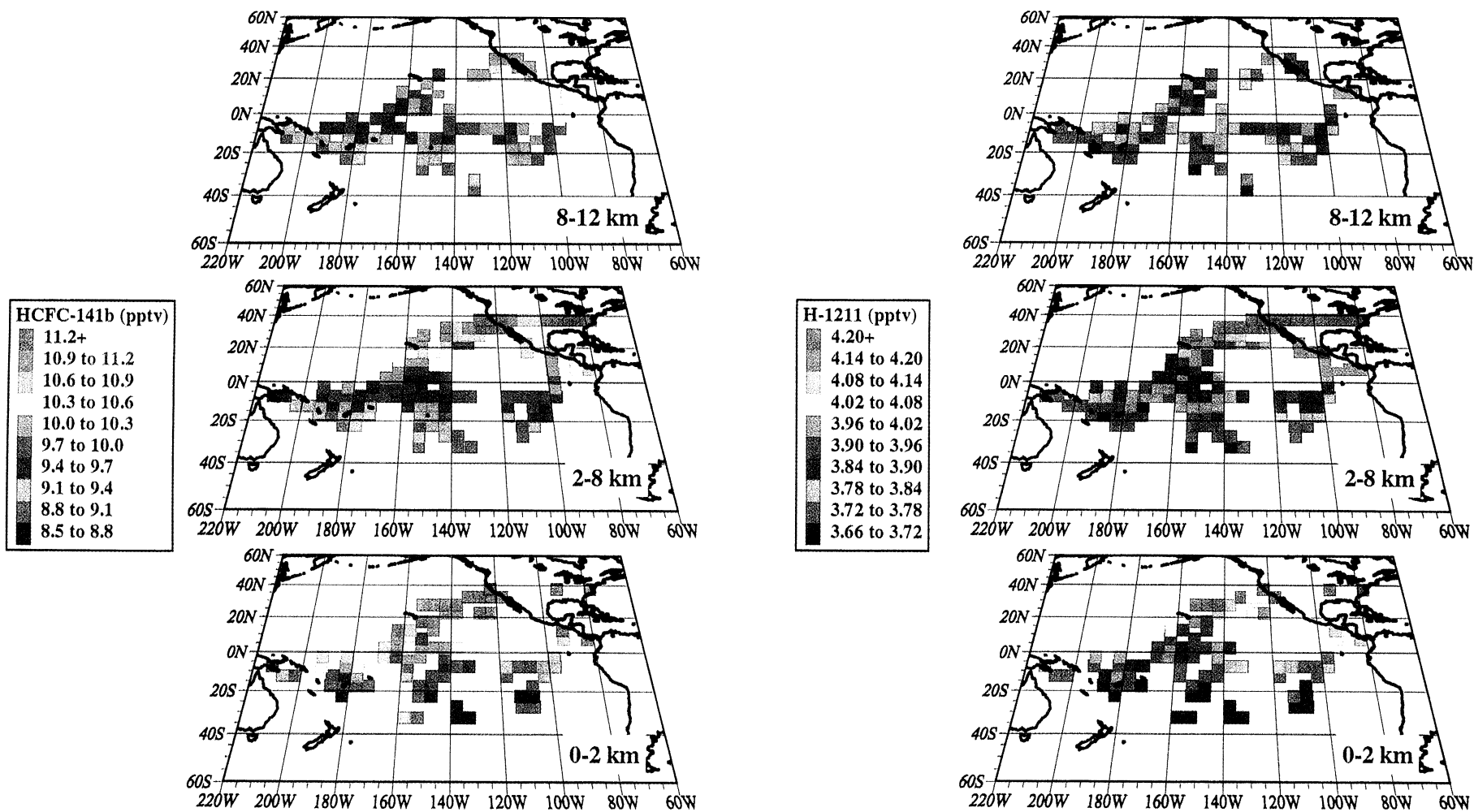- 3.78 to 3.84
- 3.72 to 3.78
- 3.66 to 3.72

Plate 1. (continued)

rapidly [*Montzka et al.*, 1999], and Halon 1211 is widely used in fire-fighting equipment.

The patch plots reveal clear interhemispheric gradients for each gas shown in Plate 1. The highest mixing ratios are observed toward the northern extent of the sampling range for each of the three altitude slices. In general, higher concentrations were also measured at lower altitudes and reached farther south with decreasing altitude. Therefore the largest north-south interhemispheric ratios were observed for the lower two altitude sections.

The greater Northern Hemisphere mixing ratios for the urban/combustion tracers ethane and propane, the fossil fuel combustion tracer ethyne, and the industrial tracers HCFC-141B, and C_2Cl_4 are consistent with their significant northern hemisphere continental urban/industrial sources. Plate 2 reveals good correlations between each of these gases and CO, especially at the lowest altitudes (<2 km), further indicating common urban/industrial sources.

The highest average Southern Hemisphere values were near the equator, where air masses characteristic of aged Northern Hemisphere air penetrated south, frequently as far as 5°S (see later). South of 10°S, average values of the trace gases shown in Plate 1 are quite low.

3.1. Signatures of Asian versus North American Air Masses

The meteorological streamlines and back trajectories presented by *Fuelberg et al.* [this issue] reveal that air sampled north of 10°N typically originated over the Asian continent, was transported eastward across the Pacific, then rotated around the North Pacific anticyclone. However, these air masses frequently grazed the coast of North America, before returning to the Pacific, heading southwest. This suggests that emissions from the US were also likely to contribute to North Pacific trace gas levels, although their relative importance is unknown. Therefore it would be useful to identify chemical signatures that could distinguish between Asian and U.S. continental air masses.

One such candidate molecule is Halon 1211 ($CBrClF_2$, a fire retardant). Current emissions of Halon 1211 are strongly associated with the Asian continent [*Fraser et al.*, 1999]. The high ozone-depleting potential of this gas (which has an ODP of 3) resulted in its regulation under the Montreal Protocol, with production ceasing in developed countries in 1994 [*United Nations Environment Programme (UNEP)*, 1991]. Thus the only sources of halons in developed countries are from halon storage "banks," including existing fire extinguishers. However, the Montreal Protocol allows developing countries such as the People's Republic of China (PRC) to have until 2010 before they must completely phase out Halon 1211 production [*UNEP*, 1991].

The atmospheric concentration of Halon 1211 has continued to grow over the past few years [*Butler et al.*, 1998; *Fraser et al.*, 1999; *Montzka et al.*, 1999]. Comparison of PEM-Tropics B with the PEM-Tropics A data in Figure 2 and Table 1 reveals an average increase of ~ 0.2 pptv/y over the 2.5 years between the 1996 and 1999 PEM-Tropics experiments. Such an increase is similar to the 0.16 and 0.21 pptv/yr reported by *Butler et al.* [1998] and *Fraser et al.* [1999], respectively for 1995-1996 and 0.20 pptv/yr for early 1998 [*Fraser et al.*, 1999]. The PRC is responsible for ~ 90 % of the world's production, so continued global growth in

atmospheric Halon 1211 mixing ratios has been attributed to increased legal manufacture and release in the PRC [*Fraser et al.*, 1999]. While some evidence of emissions from the banks would still be expected in developed countries, emissions from regions such as North America, Japan, and Europe should be relatively low.

A second useful tracer molecule is CH_3Cl. This gas is a biomass combustion (and wood fuel burning) tracer [e.g., *Rasmussen et al.*, 1980, 1982; *Blake, N. J., et al.*, 1996]. Enhancements of CH_3Cl versus CO were previously employed during PEM-West B to indicate air masses of SE Asian origin that had been influenced by biomass burning [*Blake et al.*, 1997]. Air masses observed above 2 km and south of 25°N during PEM-West B exhibited high ratios of CH_3Cl versus CO. To the north of 25°N, ratios of CH_3Cl versus CO were typically low, while ratios of ethane, propane, and C_2Cl_4 versus CO were significantly higher. *Blake et al.* [1997] attributed these different regional chemical characteristics to the dominance of urban/industrial emissions at northern latitudes. By contrast, low-latitude CO emissions were strongly influenced by biomass burning type sources. During the PEM-Tropics B, period Figure 3 shows that a considerable number of hot spots associated with active fires (but which could include some "false alarms" such as gas flares and cities) were reported for SE Asia, while the West Coast of North America and northeastern Asia experienced very few instances.

We now examine the remote northern hemisphere (>10°N) PEM-Tropics B data for evidence of the continental signatures discussed above. Plate 2 shows that enhancements of CH_3Cl and Halon 1211 versus CO were greater for the mid altitude and high altitude range compared to the low altitude subset (<2 km). The reverse is true for the urban/industrial tracers ethane, ethyne, propane, C_2Cl_4, and HCFC-141B, which display higher slopes versus CO for the low altitudes compared to mid altitude or high altitude. These distinct relationships with CO suggest that the upper and midtroposphere were more strongly influenced by a mix of biomass burning emissions and emissions of Halon 1211, possibly from SE Asia and developing countries such as the PRC. By contrast, the lower troposphere was more strongly influenced by a mix of urban/industrial emissions that did not include a large component from the PRC or from biomass burning.

To investigate further the likely origins of the signatures of these air masses, we must consider the PEM-Tropics B meteorological conditions described by *Fuelberg et al.* [this issue] in more detail. Backward trajectories and average streamlines for the midtroposphere and uppertroposphere show air masses originating from southerly regions of Asia [*Fuelberg et al.*, this issue]. These regions include the PRC and SE Asia. The higher absolute mixing ratios of Halon 1211 and CH_3Cl at mid altitudes (1-5 km) in Figure 2 also support a relatively greater mixed PRC/SE Asian biomass burning influence in the midtroposphere during PEM-Tropics B compared to the lowest altitudes.

Average streamlines and backward trajectories shown by *Fuelberg et al.* [this issue] reveal that at latitudes >10°N, low altitudes were typically under westerly flow conditions that tended to originate from mid to high northern latitudes, including Japan. The atmospheric lifetimes of the NMHCs and C_2Cl_4 are greatly lengthened (from days to weeks) in

Latitudes >10°N

Latitudes 10°N-5°S

Latitudes >10°S
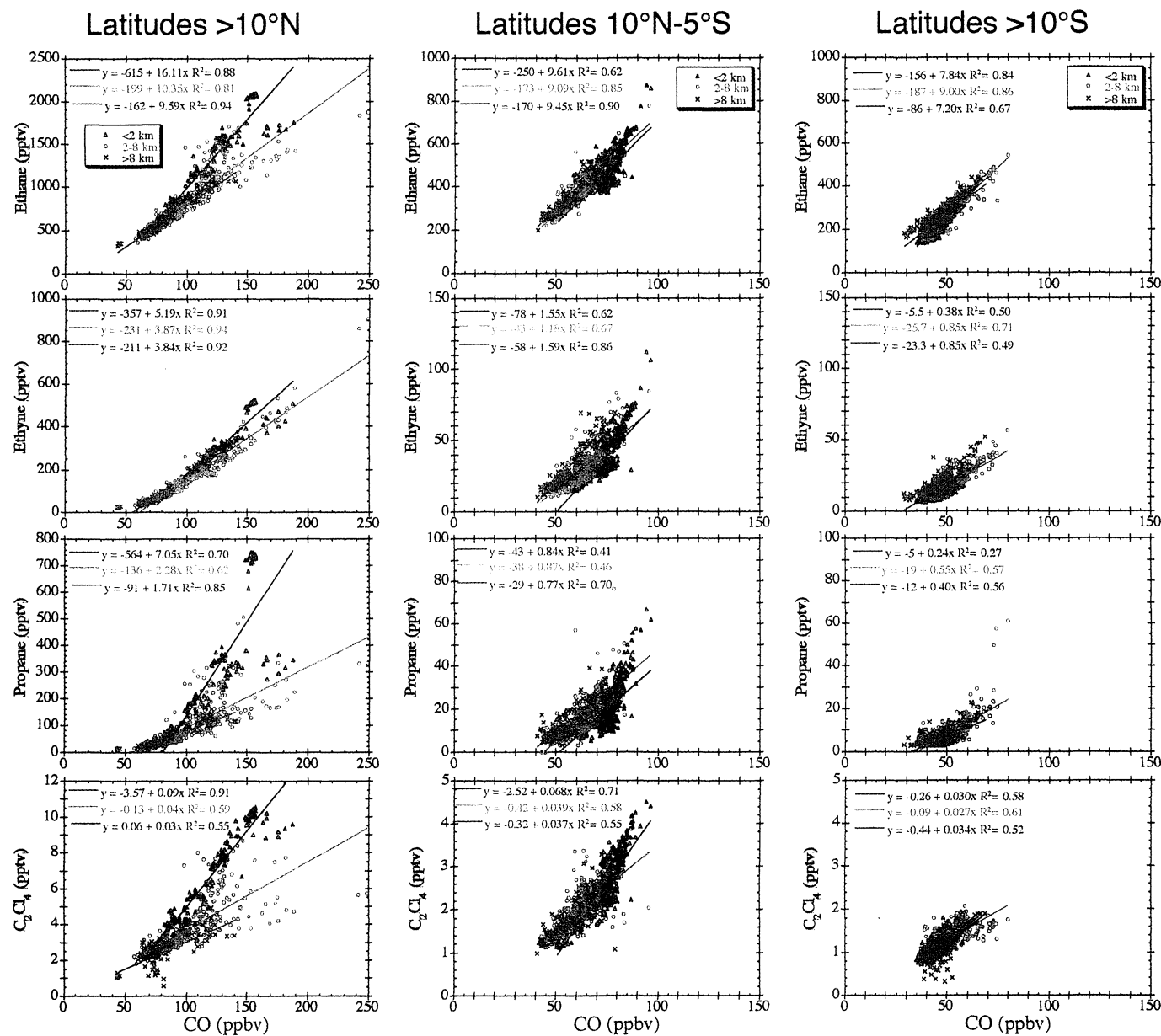
Plate 2. Correlation plots of ethane, ethyne, propane, C_2Cl_4, HCFC-141B, Halon 1211 and CH_3Cl over remote regions of the Pacific Ocean during PEM-Tropics B. The data are divided into three altitude ranges, <2 km (blue triangles), 2-8 km (green crosses), and >8 km (red circles) and three latitude ranges, >10°N, 10°N-5°S, and >10°S. Please note mixing ratio scale changes.
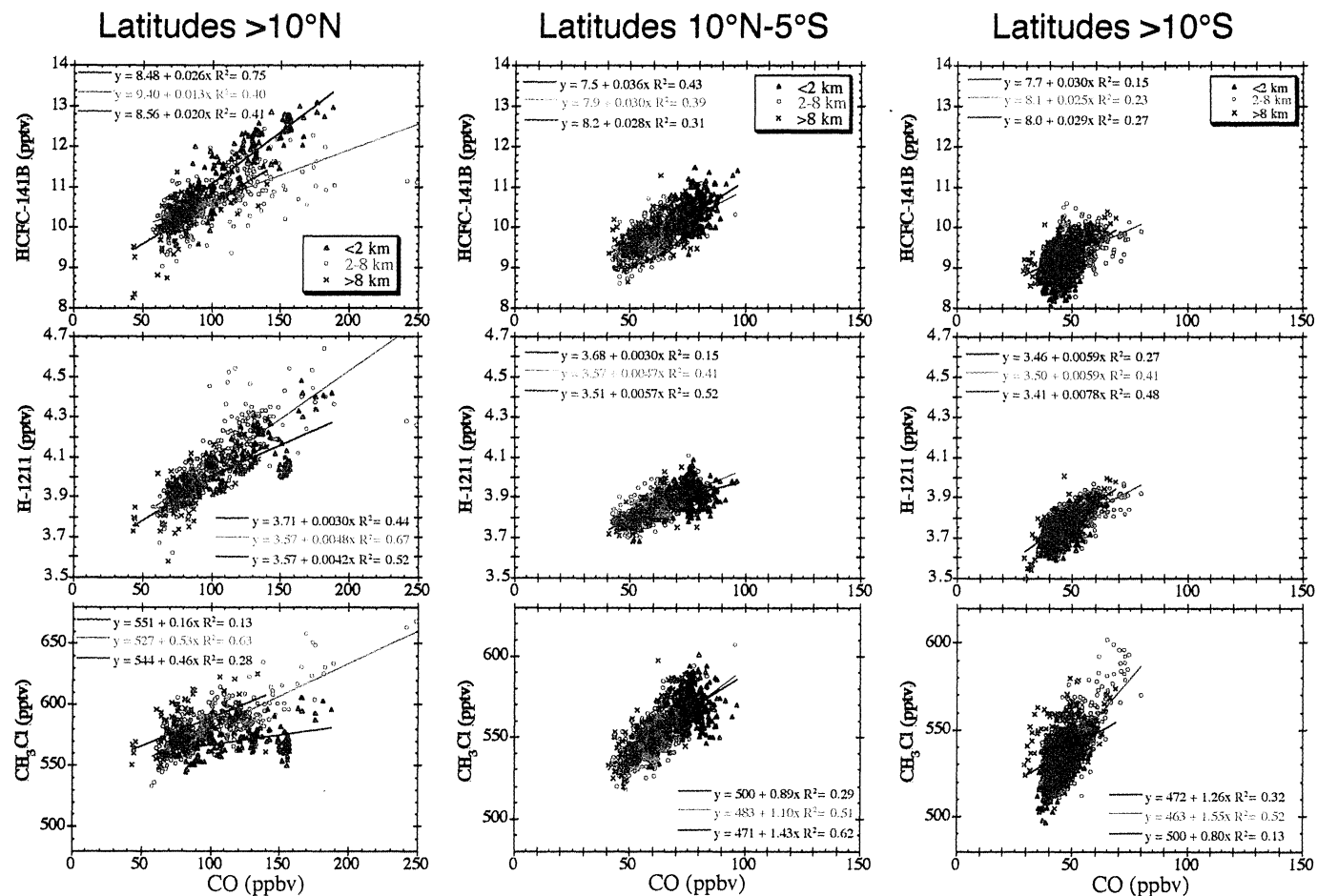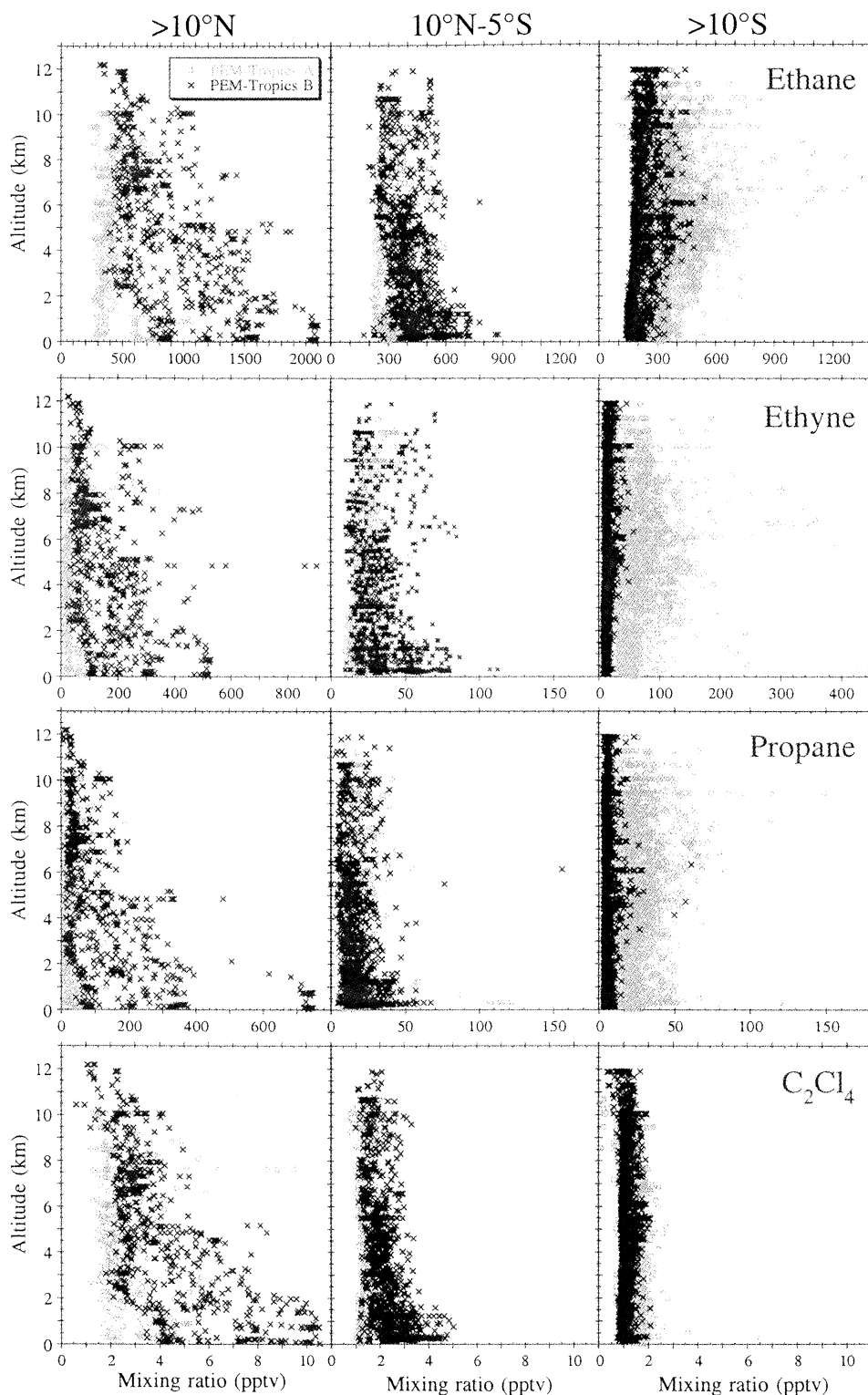
Latitudes >10°N

HCFC-141B (pptv)

$y = 8.48 + 0.026x \; R^2 = 0.75$
$y = 9.40 + 0.013x \; R^2 = 0.40$
$y = 8.56 + 0.020x \; R^2 = 0.41$

▲ <2 km
○ 2-8 km
✕ >8 km

H-1211 (pptv)

$y = 3.71 + 0.0030x \; R^2 = 0.44$
$y = 3.57 + 0.0048x \; R^2 = 0.67$
$y = 3.57 + 0.0042x \; R^2 = 0.52$

CH₃Cl (pptv)

$y = 551 + 0.16x \; R^2 = 0.13$
$y = 527 + 0.53x \; R^2 = 0.63$
$y = 544 + 0.46x \; R^2 = 0.28$

CO (ppbv)

Latitudes 10°N-5°S

HCFC-141B (pptv)

$y = 7.5 + 0.036x \; R^2 = 0.43$
$y = 7.9 + 0.030x \; R^2 = 0.39$
$y = 8.2 + 0.028x \; R^2 = 0.31$

▲ <2 km
○ 2-8 km
✕ >8 km

H-1211 (pptv)

$y = 3.68 + 0.0030x \; R^2 = 0.15$
$y = 3.57 + 0.0057x \; R^2 = 0.41$
$y = 3.51 + 0.0057x \; R^2 = 0.52$

CH₃Cl (pptv)

$y = 500 + 0.89x \; R^2 = 0.29$
$y = 483 + 1.10x \; R^2 = 0.51$
$y = 471 + 1.43x \; R^2 = 0.62$

CO (ppbv)

Latitudes >10°S

HCFC-141B (pptv)

$y = 7.7 + 0.030x \; R^2 = 0.15$
$y = 8.1 + 0.025x \; R^2 = 0.23$
$y = 8.0 + 0.029x \; R^2 = 0.27$

▲ <2 km
○ 2-8 km
✕ >8 km

H-1211 (pptv)

$y = 3.46 + 0.0059x \; R^2 = 0.27$
$y = 3.50 + 0.0059x \; R^2 = 0.41$
$y = 3.41 + 0.0078x \; R^2 = 0.48$

CH₃Cl (pptv)

$y = 472 + 1.26x \; R^2 = 0.32$
$y = 463 + 1.55x \; R^2 = 0.52$
$y = 500 + 0.80x \; R^2 = 0.13$

CO (ppbv)

Plate 2. (continued)

Figure 2. Comparison of vertical profiles of ethane, ethyne, propane, C_2Cl_4, HCFC-141B, Halon 1211, and CH_3Cl over remote regions of the Pacific Ocean during the August-September 1996 PEM-Tropics A (gray circles) and the March-April 1999 PEM-Tropics B (black crosses). The data are divided into three latitude ranges, >10°N, 10°N-5°S, and >10°S. Please note mixing ratio scale changes.

winter at high latitudes. Therefore these low altitude air masses likely represent combined emissions from the many developed nations located at mid to high northern latitudes, including Japan, Northern Europe, and North America.

As mentioned earlier, close to the coast of North America the low altitude flow becomes more northerly then northeasterly, which may allow direct mixing of emissions from North America. Such a contribution from North American air masses is supported by the trace gas composition of several samples that were collected during the P3-B Flight 4 transit to Hawaii (Figure 4). These were collected during two periods when the aircraft descended
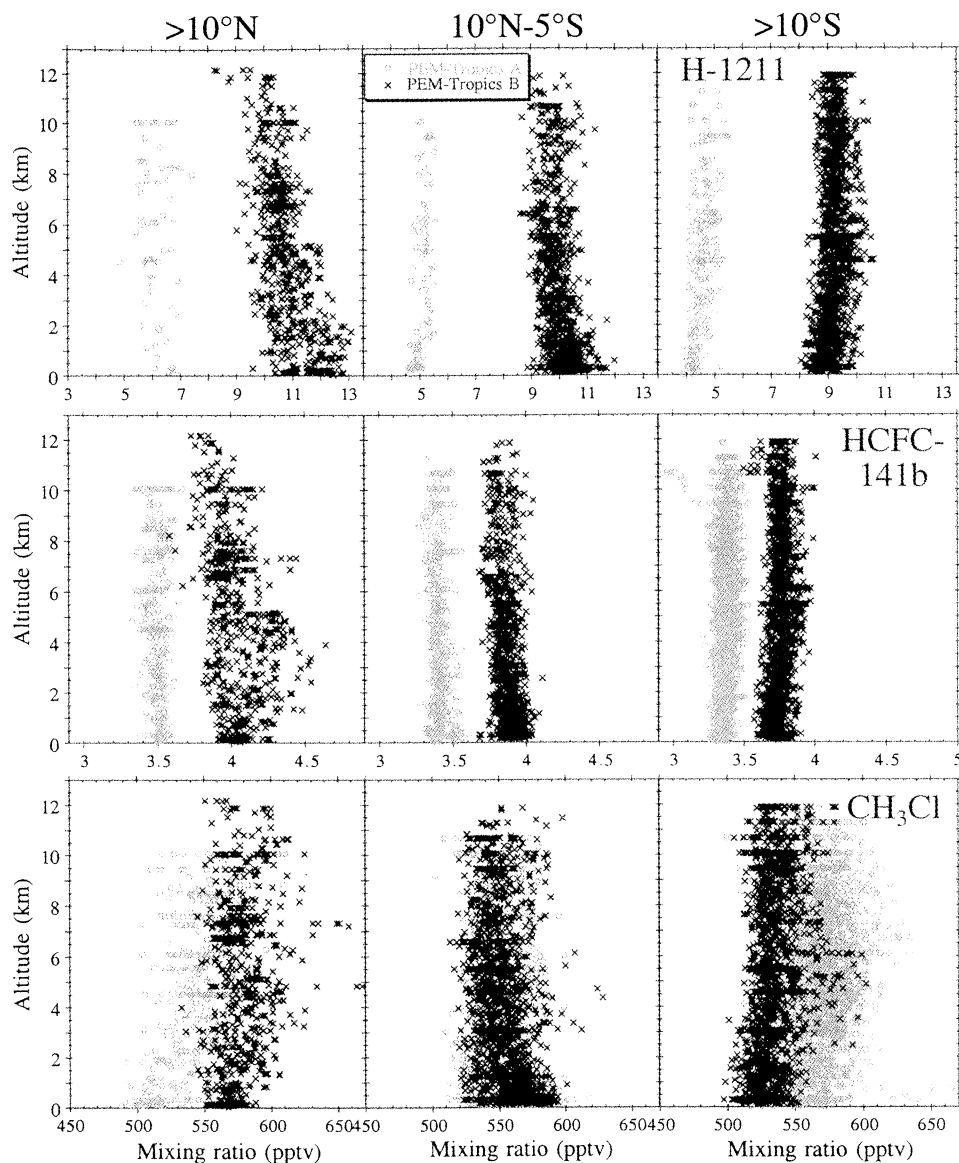
Figure 2. (continued)

below 1 km ~ 500-800 km and 1850-2300 km off the U.S. coast. Figure 4 shows that these low altitude samples exhibited high enough mixing ratios of the relatively short-lived hydrocarbon ethene (~ 10-40 pptv), to make it very unlikely that the air masses had traveled from Asia. The mixing ratios of CO were ~ 130-150 ppbv. The plumes exhibit high C_2Cl_4 (as well as ethane, ethyne, propane, and HCFC-141B) mixing ratios yet concentrations of Halon 1211 and CH_3Cl were low (Figure 4). The highly developed industrial regions of Japan, Europe, and North America have ceased production of Halon 1211, but they burn large amounts of fossil fuels and use significant quantities of C_2Cl_4 as a solvent and chemical intermediate. In addition, these regions tend to have a relatively low frequency of biomass burning/wood fuel combustion.

3.2. Central/South American Outflow

At low altitudes (<2 km) near the coast of Central America during DC-8 flights 21 and 22, elevated mixing ratios were

observed for each trace gas presented in Plate 2. Levels of short-lived ethene (not shown) were also high (near 200 pptv). This indicates that the air masses sampled in this region represented the outflow of a mix of continental pollution, including fresh emissions. Backward trajectories show that this air originated from the east over northern South America, the Caribbean, and the southeastern United States [*Fuelberg et al.*, this issue]. Therefore these samples were not included in the "remote Pacific" data shown in Table 1, Plate 2, and Figure 2.

Average mixing ratios in the mid altitude range (2-8 km) near the coast of Central America were also significantly elevated for gases characteristic of biomass burning (e.g., ethane, ethyne, and CH_3Cl). However, the industrial gases C_2Cl_4 and HCFC-141B were close to background levels. The back trajectories calculated by *Fuelberg et al.* [this issue], as well as the graphical simulation presented by Chatfield et al. (manuscript in preparation, 2001), indicate that these biomass burning emissions had been carried in the east to west trade winds from fires in northern South America (Figure 3).
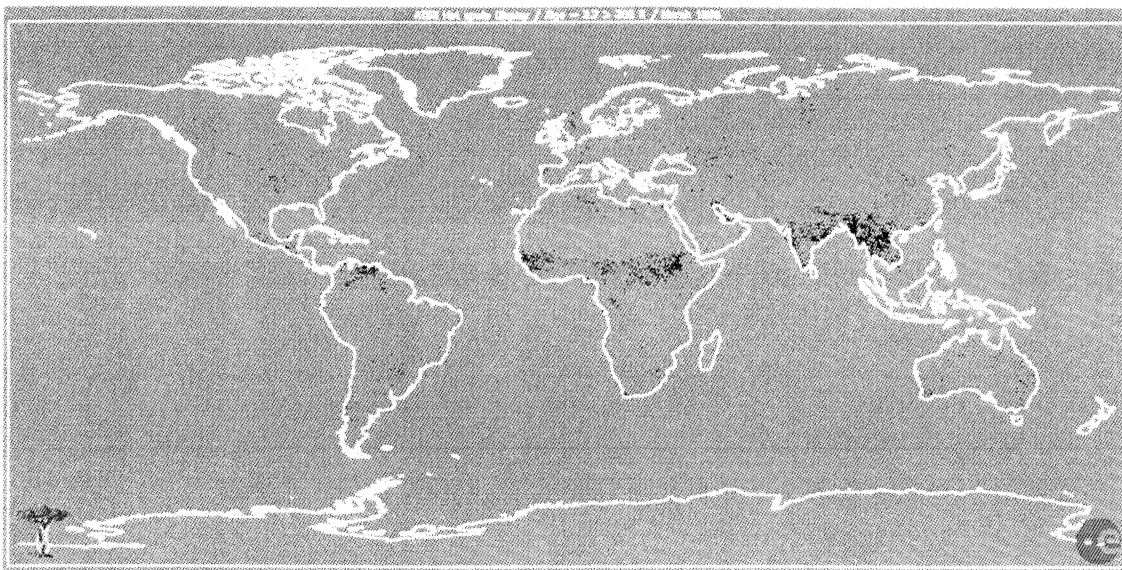
Figure 3. ATSR hot spots for March 1999 shown in black. Image taken from the ATSR World Fire Atlas, European Space Agency - ESA/ESRIN, via Galileo Galilei, CP 64, 00044 Frascati, Italy.
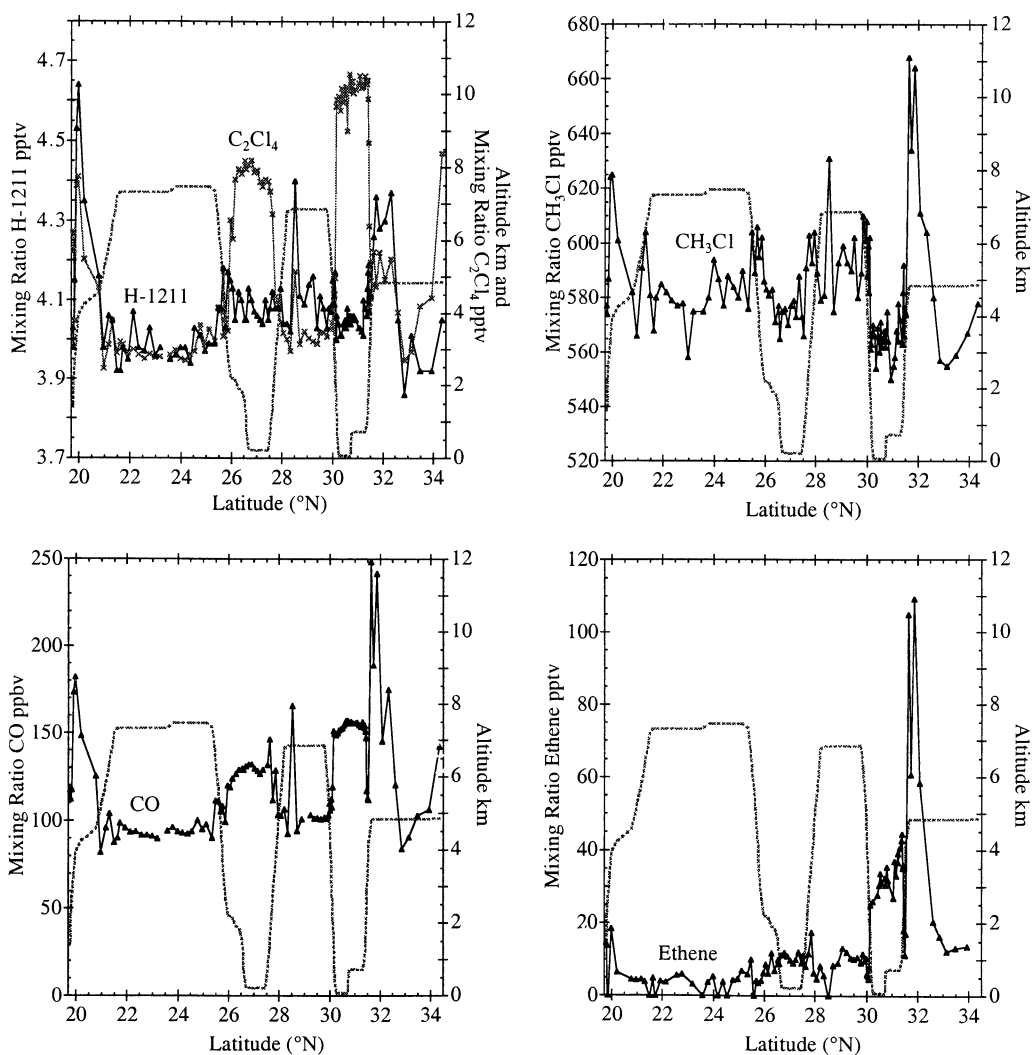
Figure 4. Latitudinal plots showing low mixing ratios of Halon 1211, and CH₃Cl, below 1 km in plumes containing high values of C₂Cl₄ and CO during P3-B Flight 4, NASA Dryden to Hilo, March 11, 1999. The broken line represents altitude.

4. Comparison of PEM-Tropics A and B

PEM-Tropics B complemented the PEM-Tropics A mission in providing an opportunity to investigate the chemical and transport properties of the tropical troposphere and make baseline measurements during a different season. PEM-Tropics A demonstrated the large impact of biomass burning emissions on the composition and chemistry of the troposphere over the South Pacific during the southern tropical dry season [e.g., Blake et al., 1999a; Schultz et al., 1998; Talbot et al., 1999]. By contrast, PEM-Tropics B took place in the southern tropical wet season, when the influence from biomass burning was predicted to be minimal.

4.1. North of 10°N

Although the main focus of both PEM-Tropics A and PEM-Tropics B was on the tropical and southern Pacific, high-latitude Northern Hemisphere emissions do impact the trace gases composition of tropical regions (Logan et al., unpublished manuscript, 2001). For example, the latitudinal distribution of ethane is influenced by interhemispheric transfer, whereby half of the ethane source in the Southern Hemisphere results from transport from the Northern Hemisphere [Rudolph, 1995].

Figure 2 and Table 1 show that north of 10°N, absolute mixing ratios of ethane, ethyne, and propane, were significantly higher for the lower two altitude ranges during PEM-Tropics B compared to PEM-Tropics A. Mixing ratios of C_2Cl_4 and CH_3Cl were also significantly greater during PEM-Tropics B at low altitudes, but only slightly higher at mid altitudes. During PEM-Tropics B the westerly transport of this pollution was strongest below ~ 5 km. As outlined in the discussion of continental outflow of trace gases above, the air masses seen at low altitude typically had high-latitude origins during PEM-Tropics B. This is consistent with the seasonal accumulation of NMHCs and C_2Cl_4, which have

long winter atmospheric lifetimes at high latitudes [e.g., Penkett et al., 1993; Wang et al., 1995]. By contrast, the timing of PEM-Tropics A coincided with the seasonal minima for these gases and encountered very clean air masses in the Northern Hemisphere (Table 1).

The altitude of continental outflow below 5 km for PEM-Tropics B is similar to the range of principal outflow observed during PEM-West B. PEM-West B took place at a comparable time of year to (February and March of 1994) but closer to the Asian Pacific Rim than PEM-Tropics B [e.g., Blake et al., 1997; Talbot et al., 1997].

4.2. Between 10°N and 5°S: Penetration of Northern Hemisphere air into the Southern Hemisphere

The vertical profiles in Figure 2 for the latitude range 10°N-5°S reveal mixing ratios above ~ 5 km for the NMHCs, C_2Cl_4, and CH_3Cl that are similar for both PEM-Tropics A and PEM-Tropics B. The average values in Table 1 support this observation. However, at altitudes below 2 km, Figure 2 and Table 1 show that the mean mixing ratios of ethane, C_2Cl_4, and CO during PEM-Tropics B are significantly higher than those for PEM-Tropics A, while O_3 is slightly lower.

Fuelberg et al. [this issue] report that during PEM-Tropics A, the ITCZ was located near 10°N and was associated with well-defined cross-equatorial flow from the Southern Hemisphere into the Northern Hemisphere. By contrast, the ITCZ was much weaker during PEM-Tropics B, with two zones of convergence. Over the central and extreme western Pacific, flow was predominantly from the northern into the southern hemisphere. The patch plots in Plate 1 clearly illustrate that towards the western extent of the sampling region, low altitude enhancements in the long-lived Northern Hemisphere tracers ethane, C_2Cl_4, and HCFC-141B persist beyond 5°S (Plate 1).

Plate 3 demonstrates this north-south air mass penetration with several vertical profiles sampled at different latitudes and
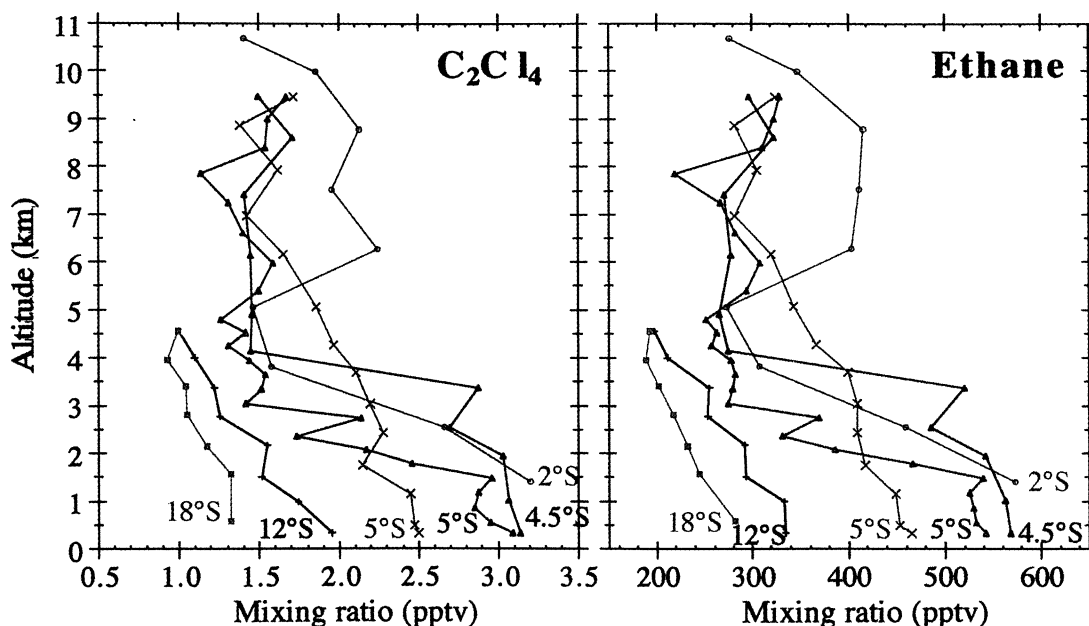
Plate 3. Vertical profiles of C_2Cl_4 and ethane, sampled during DC-8 flight 12 extending north of Fiji to 2°S on March 25, 1999.

longitudes during DC-8 Flight 12, which flew north from Fiji to 2°S on March 25, 1999. In this example, each of the vertical profiles sampled at 5°S, 4.5°S, and 2°S exhibit enhanced mixing ratios of ethane, and the industrial tracer C_2Cl_4 below ~ 3 km. These enhancements typically represent approximately twice the concentration of samples collected at 18°S, which can be considered representative of the clean "background" Southern Hemisphere troposphere during this time of year (Table 1). The area near the equator was under easterly flow during this flight. The 10-day backward trajectories show that the air arriving at flight level originated northeast of the flight track but had remained over the tropical Pacific during the previous 10 days [Fuelberg et al., this issue].

Figure 2 and Table 1 show that near the equator there was almost no enhancement of propane, and only slight enhancement in ethyne, during PEM-Tropics B compared to PEM-Tropics A, even at low altitude. Plate 2 further reveals that for the latitude range 10°N-5°S the slopes for the correlations between ethyne and CO, and propane and CO are very low during PEM-Tropics B. Both NMHCs have atmospheric lifetimes significantly less than CO, so their mixing ratios would decrease faster than CO as the result of photochemical aging and mixing. Therefore these observations indicate that the low altitude air in this region was significantly aged.

The aged nature of this equatorial air makes it extremely difficult to pick out any continental signature such as those described above, so we were unable to determine a likely specific continental origin for these air masses. All that we can state at this time is that they retain enhancements of urban and industrial emissions (such as ethane, C_2Cl_4, and HCFC-141B), which are characteristic of the Northern Hemisphere.

4.3. South of 10°S

Table 1 reveals that south of 10°S, average mixing ratios for ethane, ethyne, propane, CH_3Cl, CO, and O_3 were significantly lower at all altitudes during PEM-Tropics B compared to PEM-Tropics A, except for O_3 at high altitude. For example, ethyne mixing ratios were only ~ 20% of PEM-Tropics A levels in the mid altitude range. By contrast, the mean mixing ratios of C_2Cl_4 are only slightly lower.

Figure 2 clearly illustrates the high mid altitude mixing ratios for ethane, ethyne, and CH_3Cl from the many biomass burning plumes that were encountered during PEM-Tropics A [see also Blake et al., 1999a]. During PEM-Tropics B the South Pacific Convergence Zone extended northwest to southeast near New Guinea, blending into the ITCZ to the north (see Figure 1). Trajectory analyses indicate that the air sampled south of 10°S but north of the SPCZ had a long residence time over the Pacific and most likely originated from South America several weeks before [Fuelberg et al.,
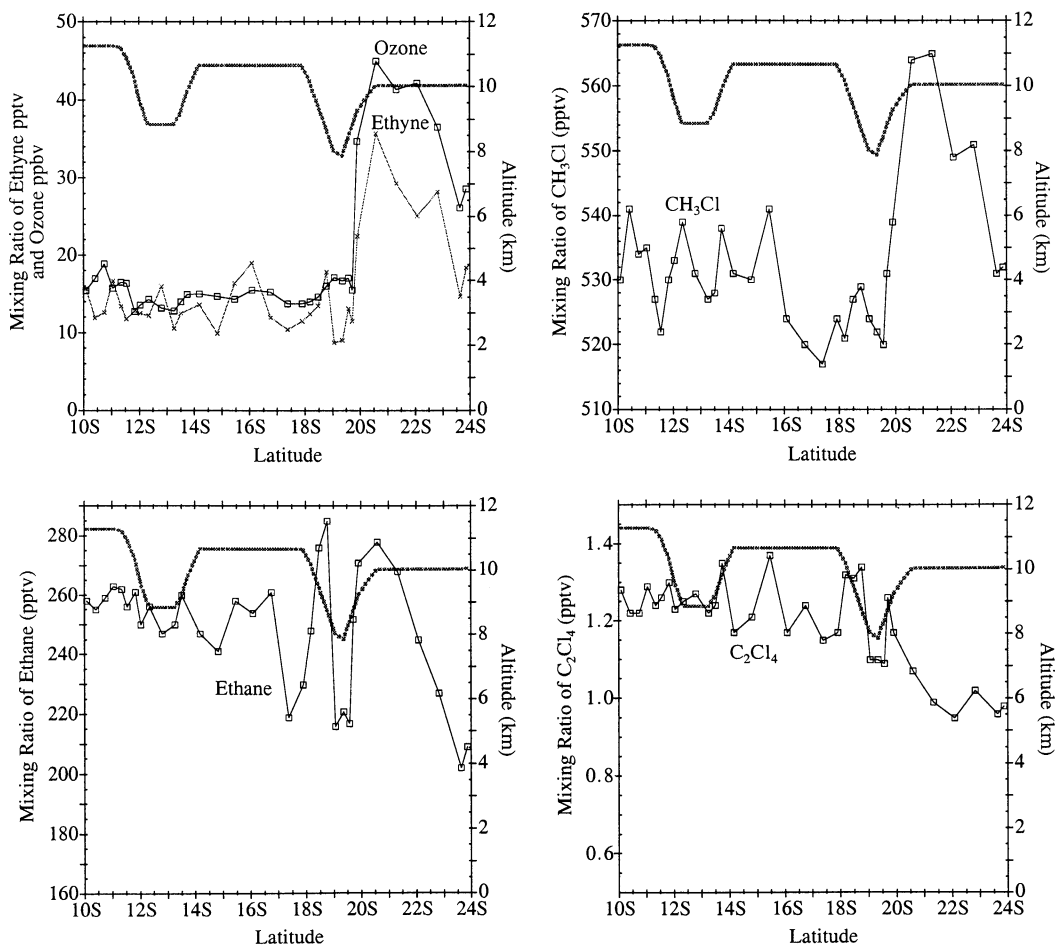
Figure 5. Latitudinal gradients of O_3, ethyne, ethane, CH_3Cl, and C_2Cl_4 as the DC-8 crossed the SPCZ to the north of Fiji on March 20, 1999 (flight 10). The broken line represents altitude.

Table 1. Comparison of PEM-Tropics A (PTA) With PEM-Tropics B (PTB) Mixing Ratios in Parts per Trillion by Volume (pptv), Except Where Indicated, for Three Latitude Regions of the Remote Pacific[a]

	Ethane		Ethyne		Propane		C_2Cl_4		CH_3Cl		CH_3Br		CH_3I		HCFC-141B		H-1211		CO ppbv		O_3 ppbv	
	PTA	PTB	PTA	PTB	PTA	PTB	PTA	PTB	PTA	PTB	PTA	PTB	PTA	PTB	PTA[b]	PTB	PTA	PTB	PTA	PTB	PTA	PTB
Latitudes >10°N																						
8-12.2 km. N=83, 111																						
Mean	454	616	70	100	41	48	2.5	2.5	557	581	10.1	9.2	0.08	0.12	6.1	10.2	3.50	3.92	70	81	51	48
SD	127	188	70	76	28	36	1.0	0.8	23	17	0.7	0.4	0.04	0.05	0.5	0.6	0.07	0.11	21	19	36	22
Median	428	554	31	70	34	35	2.0	2.5	558	579	10.2	9.1	0.07	0.11	6.1	10.2	3.51	3.91	57	76	41	44
2-8 km. N=234, 418																						
Mean	387	808	37	145	25	85	2.6	3.6	548	579	10.0	9.5	0.11	0.13	6.1	10.6	3.49	4.04	62	97	35	43
SD	99	311	31	106	19	77	1.1	1.3	18	18	0.8	0.5	0.09	0.08	0.5	0.5	0.06	0.16	12	27	14	15
Median	362	676	25	100	20	49	2.3	3.0	548	577	9.9	9.4	0.08	0.11	6.0	10.6	3.48	3.98	57	87	32	42
0-2 km. N=90, 164																						
Mean	487	1316	50	264	33	276	3.3	6.7	520	571	10.5	10.0	0.48	0.49	6.3	11.6	3.50	4.07	77	120	18	39
SD	214	455	37	143	27	222	1.1	2.4	16	12	0.7	0.5	0.25	0.18	0.4	0.8	0.04	0.12	20	27	8	12
Median	365	1300	33	238	21	211	3.2	6.3	517	570	10.8	10.0	0.54	0.52	6.3	11.7	3.51	4.05	70	118	16	39
Latitudes 10°N-5°S																						
8-12 km. N=81, 113																						
Mean	306	369	29	33	19	15	1.4	1.8	547	553	8.7	8.7	0.09	0.09	5.3	9.8	3.40	3.83	57	57	30	28
SD	41	95	9	17	6	9	0.3	0.5	17	17	0.5	0.5	0.05	0.04	0.2	0.5	0.05	0.07	5	9	6	9
Median	299	335	28	25	19	11	1.4	1.7	547	550	8.7	8.7	0.07	0.09	5.3	9.8	3.39	3.82	57	54	28	27
2-8 km. N=253, 531																						
Mean	347	381	22	29	18	15	1.5	2.0	552	550	8.8	8.6	0.09	0.12	5.2	9.8	3.41	3.86	56	61	30	21
SD	77	84	6	12	7	10	0.3	0.4	17	13	0.5	0.4	0.06	0.06	0.2	0.4	0.05	0.06	5	9	9	7
Median	341	376	21	27	17	13	1.4	2.0	552	549	8.8	8.6	0.07	0.11	5.2	9.8	3.40	3.86	55	61	31	21
0-2 km. N=258, 554																						
Mean	297	470	19	38	17	20	1.3	2.6	553	565	8.5	8.9	0.34	0.35	4.9	10.3	3.41	3.90	58	74	14	8
SD	44	101	7	16	18	10	0.2	0.7	17	13	0.4	0.5	0.12	0.15	0.2	0.5	0.05	0.06	6	7	5	3
Median	297	433	18	32	14	17	1.3	2.5	553	566	8.5	9.0	0.35	0.37	4.9	10.2	3.40	3.90	58	75	12	7
Latitudes >10°S																						
8-12 km. N=454, 497																						
Mean	377	241	60	15	27	5	1.2	1.1	567	536	8.6	8.1	0.06	0.09	4.8	9.3	3.37	3.76	64	46	60	28
SD	133	48	35	7	16	3	0.3	0.2	19	12	0.4	0.3	0.04	0.07	0.3	0.3	0.08	0.06	15	6	43	18
Median	353	232	54	13	24	5	1.3	1.1	567	535	8.6	8.1	0.06	0.08	4.7	9.3	3.38	3.76	62	45	47	24
2-8 km. N=1366, 840																						
Mean	401	240	70	15	26	6	1.4	1.2	567	536	8.7	8.1	0.08	0.12	4.7	9.3	3.38	3.77	70	48	53	23
SD	127	69	42	7	11	5	0.3	0.3	19	15	0.5	0.3	0.06	0.08	0.3	0.4	0.05	0.06	17	7	19	7
Median	368	215	62	12	24	5	1.4	1.2	568	533	8.7	8.1	0.06	0.10	4.7	9.2	3.38	3.77	65	46	51	23
0-2 km. N=378, 445																						
Mean	320	185	56	11	26	5	1.6	1.1	557	527	8.2	7.8	0.35	0.46	4.3	9.0	3.36	3.72	60	44	30	15
SD	49	41	32	3	12	3	0.4	0.2	21	11	0.4	0.3	0.16	0.18	0.2	0.4	0.04	0.06	10	5	7	4
Median	315	167	52	10	23	5	1.5	1.0	555	526	8.2	7.8	0.37	0.44	4.3	8.9	3.36	3.71	57	43	29	16

[a]Number of UCI whole air samples collected during PTA and PTB, respectively

[b]Results of analysis of subset of samples by Elliot Atlas

this issue]. In contrast, the air south of the SPCZ came rapidly from the west with an origin over Australia or Africa where very few fire hot spots were observed (Figure 3). Therefore the trace gas composition of the troposphere during PEM-Tropics B was, in general, much less influenced by long-range transport of biomass burning products than PEM-Tropics A.

Nevertheless, a few relatively small biomass burning/continental plumes were observed in the deep Southern Hemisphere. Figure 5 shows results from part of the DC-8 flight to the north of Fiji on March 20, 1999 (flight 10). As the aircraft crossed the SPCZ, which consisted of a major line of intense convection extending approximately west to east, just north of Fiji, a distinct air mass transition was

observed. The air that was sampled south of ~ 20°S, contained more than twice the mixing ratios of ozone and ethyne, together with enhanced ethane, and CH_3Cl, but lower C_2Cl_4 (Figure 5). This trace gas signature indicated that the air mass to the south of the SPCZ had previously been influenced by biomass burning emissions. Backward trajectories for the northern part of the flight originate northeast of the flight track over the southern equatorial Pacific. By contrast, the southern air masses originate south or southwest of the flight track, extending back over Australia and almost to southern Africa during the previous 10 days [*Fuelberg et al.,* this issue].

The SPCZ was located further to the west during PEM-Tropics B compared to its position near Tahiti during PEM-Tropics A [*Fuelberg et al.,* this issue]. As for PEM-Tropics A, the SPCZ provided a barrier to pollution entering the South Pacific region from the west during PEM-Tropics B [*Gregory et al.,* 1999; *Avery et al.,* this issue]. Therefore its more westerly position appears to have contributed to the relatively "pristine" average trace gas mixing ratios observed over the South Pacific during PEM-Tropics B. These different conditions in turn significantly altered the photochemical environment, including the photochemical budgets of HO_X, NO_X, and O_3 [*Olson et al.,* this issue].

4.4. Latitudinal Gradients

The vertical profiles shown in Figure 2 for ethane, ethyne, propane, and C_2Cl_4 exhibit a much stronger latitudinal gradient during PEM-Tropics B than our observations made in late August to early October for PEM-Tropics A. For example, the mean mixing ratios in Table 1 reveal that the low altitude (<2 km) north-south ratio (>10°N vs. >10°S) for ethane of 1.5 during PEM-Tropics A increased to 7.1 for PEM-Tropics B. Similarly, the interhemispheric ratios increased from ~ 1 to 24 for ethyne, and from 1 to 55, and 2 to 6 for propane and C_2Cl_4, respectively.

Changes in the interhemispheric gradient with season are driven by seasonal variations of OH radicals. Alkane mixing ratios are highest in the Northern Hemisphere during the Northern Hemisphere winter because of decreased removal by OH and consequent accumulation of the large Northern Hemisphere emissions. The seasonally strong Asian continental outflow [e.g., *Talbot et al.,* 1997; *Blake et al.,* 1997] also contributes to high Northern Hemisphere concentrations. In addition, this period coincides with low summer values in the southern hemisphere, further accentuating the contrast between the two hemispheres.

As stated above, the low frequency of Southern Hemisphere biomass fires (Figure 3) contributed to the significantly lower Southern Hemisphere PEM-Tropics B mixing ratios, of the NMHCs and CH_3Cl in the midtroposphere, compared with PEM-Tropics A (Table 1). Table 1 shows that during PEM-Tropics A the midtropospheric mean value for ethyne in the Southern Hemisphere of 70±42 pptv was higher than the Northern Hemisphere value of 37±31 pptv. By contrast, the Southern Hemispheric C_2Cl_4 mean values were significantly lower than observed in the Northern Hemisphere. This observation again highlights the relatively large influence that Southern Hemisphere biomass burning emissions played in the spatial distribution of trace gases during PEM-Tropics A compared to PEM-Tropics B.

5. Conclusions

The PEM-Tropics B interhemispheric gradient was much stronger than during PEM-Tropics A. The different air masses observed over the North Pacific frequently were associated with distinct source regions and photochemical conditions. Flow from the west brought air containing mixing ratios of trace gases that were significantly higher than reported for PEM-Tropics A. These pollution levels were most elevated below ~ 5 km, and many 10-day backward trajectories originated over the Asian continent. Above about 1 km these air masses contained chemical signatures characteristic of biomass burning and emissions of Halon 1211 associated with developing nations. These backward trajectories typically originated over southern Asian regions. By contrast, air at the lowest altitudes often originated from higher northern latitudes and had characteristics of emissions from developed nations such as Japan, northern Europe, and North America.

We frequently observed penetration of aged Northern Hemisphere air into the Southern Hemisphere at low altitude to about 5°S. However, the influence of biomass burning on the trace gas composition of the majority of the Southern Hemisphere was very much diminished compared to PEM-Tropics A. The westerly position of the SPCZ during PEM-Tropics B also appears to have contributed a barrier to transport of such pollution from the west. Therefore the conditions encountered over the South Pacific during PEM-Tropics B were considerably more characteristic of the minimally polluted remote marine environment, providing a background with which to compare and quantify future human induced changes.

References

Apel, E. C., J. G. Calvert, and F. C. Fehsenfeld, The Nonmethane Hydrocarbon Intercomparison Experiment (NOMHICE): Tasks 1 and 2, *J. Geophys. Res., 99,* 16,651-16,664, 1994.

Apel, E. C., J. G. Calvert, T. M. Gilpin, F. C. Fehsenfeld, The Nonmethane Hydrocarbon Intercomparison Experiment (NOMHICE): Task 3, *J. Geophys. Res., 104,* 26,069-26,086, 1999.

Atlas, E., W. Pollock, J. Greenberg, L. Heidt, and A. M. Thompson, Alkyl nitrates, nonmethane hydrocarbons, and halocarbon gases over the equatorial Pacific Ocean during SAGA 3, *J. Geophys. Res., 98,* 16,933-16,949, 1993.

Avery, M. A., D. J. Westberg, R. E. Newell, H. E. Fuelberg, B. E. Anderson, J. D. Barrick, S. A. Vay, G. W. Sachse, and G. L. Gregory, A comparison of altitude-dependent chemical tracer transport across persistent tropical convective zones during PEM-Tropics missions A and B, *J. Geophys. Res.,* this issue.

Blake, D. R., and F. S. Rowland, Global atmospheric concentrations and source strengths of ethane, *Nature, 321,* 231-233, 1986.

Blake, D. R., and F. S. Rowland, Urban leakage of liquefied petroleum gas and its impact on Mexico City air quality, *Science*, *269*, 953-956, 1995.

Blake, D. R., D. F. Hurst, T. W. Smith Jr., W. J. Whipple, T.-Y. Chen, N. J. Blake, and F. S. Rowland, Summertime measurements of selected nonmethane hydrocarbons in the Arctic and subarctic during the 1988 Arctic Boundary Layer Expedition (ABLE-3A), *J. Geophys. Res.*, *97*, 16,559-16,588, 1992.

Blake, D. R., T. W. Smith Jr., T.-Y. Chen, W. J. Whipple, and F. S. Rowland, Effects of biomass burning on summertime nonmethane hydrocarbon concentrations in the Canadian wetlands, *J. Geophys. Res.*, *99*, 1,699-1,719, 1994.

Blake, D. R., T. Y. Chen, T. W. Smith Jr., C. J.-L. Wang, O. W. Wingenter, N. J. Blake, F. S. Rowland, and E. W. Mayer, Three-dimensional distribution of NMHCs and halocarbons over the northwestern Pacific during the 1991 Pacific Exploratory Mission (PEM-West A), *J. Geophys. Res.*, *101*, 1763-1778, 1996.

Blake, N. J., D. R. Blake, B. C. Sive, T.-Y. Chen, J. E. Collins Jr., G. W. Sachse, B. E. Anderson, and F. S. Rowland, Biomass burning emissions and vertical distribution of atmospheric methyl halides and other reduced carbon gases in the South Atlantic Region, *J. Geophys. Res.*, *101*, 24,151-24,164, 1996.

Blake, N. J., D. R. Blake, T.-Y. Chen, J. E. Collins Jr., G. W. Sachse, B. E. Anderson, and F. S. Rowland, Distribution and seasonality of selected hydrocarbons and halocarbons over the western Pacific basin during PEM-West A and PEM-West B, *J. Geophys. Res.*, *102*, 28,315-28,331, 1997.

Blake, N. J., et el., Influence of southern hemispheric biomass burning on mid-tropospheric distributions of nonmethane hydrocarbons and selected halocarbons over the remote South Pacific, *J. Geophys. Res.*, *104*, 16,213-16,232, 1999a.

Blake, N. J., et al., Aircraft measurements of the latitudinal, vertical, and seasonal variations of NMHCs, methyl nitrate, methyl halides, and DMS during the First Aerosol Characterization Experiment (ACE 1), *J. Geophys. Res.*, *104*, 21,803-21,817, 1999b.

Bonsang, B., and C. Boissard, Global distributions of reactive hydrocarbons in the atmosphere, in *Reactive Hydrocarbons in the Atmosphere*, edited by C. N. Hewitt, pp. 209-265, Academic, San Diego, Calif., 1999.

Butler, J. H., J. W. Elkins, T. M. Thompson, B. D. Hall, S. O. Cummings, and S. A. Montzka, A decrease in the growth rates of atmospheric halon concentrations, *Nature, 359*, 403-405, 1992.

Butler, J. H., S. A. Montzka, A. D. Clarke, J. M. Lobert, and J. W. Elkins, Growth and distribution of halon in the atmosphere, *J. Geophys. Res.*, *103*, 1503-1511, 1998.

Crutzen, P. J., A discussion of the chemistry of some minor constituents in the stratosphere and troposphere, *Pure Appl. Geophys.*, *106-108*, 1385-1399, 1973.

Donahue, N. M., and R. G. Prinn, In situ nonmethane hydrocarbon experiments on SAGA 3, *J. Geophys. Res.*, *98*, 16,915-16,932, 1993.

Fraser, P. J., D. E. Oram, C. E. Reeves, S. A. Penkett, and A. McCulloch, Southern Hemispheric halon trends (1978-1998) and global halon emissions, *J. Geophys. Res.*, *104*, 15,985-15,999, 1999.

Fuelberg, H. E., R. E. Newell, D. J. Westberg, J. C. Maloney, J. R. Hannan, B. D. Martin, M. A. Avery, and Y. Zhu, A meteorological overview of the second Pacific Exploratory Mission in the Tropics, *J. Geophys. Res.*, this issue.

Greenberg, J. P., Helming, D., and P. R. Zimmerman, Seasonal measurements of non methane hydrocarbons and carbon monoxide at the Mauna Loa observatory during the Mauna Loa Observatory Photochemistry Experiment 2, *J. Geophys. Res.*, *101*, 14,581-14,598, 1996.

Gregory, G, L., D. J. Westberg, M. C. Shipman, D. R. Blake, R. E. Newell, R. W. Talbot, B. G. Heikes, G. W. Sachse, B. E. Anderson, and D. C. Thornton, Chemical characteristics of Pacific tropospheric air in the region of the ITCZ and SPCZ, *J. Geophys. Res.*, 104, 5677-5696, 1999.

Gregory, G.L., C.H. Hudgins, J. Ritter, and M. Lawrence, In situ ozone instrumentation for 10-Hz measurements: Development and evaluation, in *Proceedings of Sixth Symposium on Meteorological Observations and Instrumentation* pp., 136-139, American Meteorological Society, Boston, Mass.,1987.

Hoell, J. M., Jr., D. D. Davis, D. J. Jacobs, M. O. Rodgers, R. E. Newell, H. E. Fuelberg, R. J. McNeal, J. L. Raper, and R. J.

Bendura, Pacific Exploratory Mission in the Tropical Pacific: PEM Tropics A, August-September 1996, *J. Geophys. Res.*, *104*, 5567-5583, 1999.

Matsueda, H., H. Y. Inoue, Y. Sawa, Y. Tsutsumi, and M. Ishii, Carbon monoxide in the upper troposphere over the western Pacific between 1993 and 1996, *J. Geophys. Res.*, *103*, 19,093-19,110, 1998.

Montzka, S. A., et al., Present and future trends in the atmospheric burden of ozone-depleting halogens, *Nature 398*, 690-694, 1999.

Olson, J. R., et al., Seasonal differences in the photochemistry of the South Pacific: A comparison of observations and model results from PEM-Tropics A and B, *J. Geophys. Res.*, this issue.

Penkett, S. A., N. J. Blake, P. Lightman, A. R. W. Marsh, P. Anwyl, and G. Butcher, The seasonal variation of non-methane hydrocarbons in the free troposphere over the North Atlantic Ocean: Possible evidence for extensive reaction of hydrocarbons with the nitrate radical, *J. Geophys. Res.*, *98*, 2865-2885, 1993.

Raper, J., M. Kleb, D. J. Jacobs, D. D. Davis, R. Newell, H. Fuelberg, R. Bendura, J. Hoell, and R. McNeal, Pacific Exploratory Mission in the tropical Pacific: PEM-Tropics-B, March-April, 1999, *J. Geophys. Res.*, this issue.

Rasmussen, R. A., L. E. Rasmussen, M. A. K. Khalil, and R. W. Dalluge, Concentration distribution of methyl chloride in the atmosphere, *J. Geophys. Res.*, *85*, 7350-7356, 1980.

Rasmussen, R. A., M. A. K. Khalil, and J. S. Chang, Atmospheric trace gases over China, *Environ. Sci. Technol.*, *16*, 124-126, 1982.

Ridley, B. A., E. L. Atlas, J. G. Walega, G. L. Kok, T. A. Staffelbach, J. P. Greenberg, F. E. Grahek, P. G. Hess and D. D. Montzka, Aircraft measurements made during the spring maximum of ozone over Hawaii: Peroxides, CO, O_3, NO_Y, condensation nuclei, selected hydrocarbons, halocarbons, and alkyl nitrates between 0.5 and 9 km, *J. Geophys. Res.*, *102*, 18,935-18,961, 1997.

Rudolph, J., The tropospheric distribution and budget of ethane, *J. Geophys. Res.*, *100*, 11,369-11,383, 1995.

Rudolph, J., A. Khedim, and D. Wagenbach, The seasonal variation of light nonmethane hydrocarbons in the Antarctic troposphere, *J. Geophys. Res.*, *94*, 13,039-13,044, 1989.

Rudolph, J., A. Khedim, T. Clarkson, and B. Wagenbach, Long-term measurements of light alkanes and acetylene in the Antarctic troposphere, *Tellus, Ser. B, 44*, 252-261, 1992.

Sachse, G. W., J. E. Collins Jr., G. F. Hill, L. O. Wade, L. G. Burney, and J. A. Ritter, Airborne tunable diode laser system for high precision concentration and flux measurements of carbon monoxide and methane, *Proc. SPIE Int. Opt. Eng.*, *1433*, 145-156, 1991.

Schultz, M. G., et al., On the origin of tropospheric ozone and NO_X over the tropical South Pacific, *J. Geophys. Res.*, *104*, 5829-5844, 1999.

Seinfeld, J. H., and S. N. Pandis, *Atmospheric Chemistry and Physics*, John Wiley, New York, 1998.

Simpson, I. J., J. J. Colman, A. L. Swanson, A. R. Bandy, D. C. Thornton, D. R. Blake, and F. S. Rowland, Aircraft measurements of dimethyl sulfide (DMS) using a whole air sampling technique, *J. Atmos. Chem, 39*, 191-213, 2001.

Singh, H. B., and L. J. Salas, Measurements of selected light hydrocarbons over the Pacific Ocean, *Geophys. Res. Lett.*, *9*, 842-845, 1982.

Singh, H. B., W. Viezee, and L. J. Salas, Measurements of selected C_2-C_5 hydrocarbons in the troposphere: Latitudinal, vertical and temporal variations, *J. Geophys. Res.*, *93*, 15,861-15,878, 1988.

Sive, B. C., Atmospheric NMHCs: Analytical methods and estimated hydroxyl radical concentrations, Ph.D. thesis, Univ. of Calif., Irvine, 1998.

Sive, B. C, D. R. Blake, and F. S. Rowland, High precision simultaneous multi-column gas chromatographic analysis of atmospheric nonmethane hydrocarbons, halocarbons, and alkyl nitrates in remote environments, *in preparation*.

Smyth, S., et al., Comparison of free tropospheric western Pacific air mass classification schemes for the PEM-West A experiment, *J. Geophys. Res.*, *101*, 1743-1762, 1996.

Talbot, R. W., et al., Chemical characteristics of continental outflow from Asia to the troposphere over the western Pacific Ocean during February - March 1994: Results from PEM-West B, *J. Geophys. Res.*, *102*, 28,255-28,274, 1997.

Talbot, R. W., J. E. Dibb, E. M. Scheuer, D. R. Blake, N. J. Blake, G.

L. Gregory, G. W. Sachse, J. D. Bradshaw, S. T. Sandholm, and H. B. Singh, Influence of biomass burning combustion emissions on the distribution of acidic trace gases over the southern Pacific basin during austral springtime, *J. Geophys. Res., 104*, 5623-5634, 1999.

United Nations Environment Programme (UNEP), *Handbook for the Montreal Protocol on Substances that Deplete the Ozone Layer*, 2nd Ed., Ozone Secr., Nairobi, Kenya, 1991.

Wang, C. J.-L., D. R. Blake, and F. S. Rowland, Seasonal variations in the atmospheric distribution of a reactive chlorine compound, tetrachloroethene ($CCl_2=CCl_2$), *Geophys. Res. Lett., 22*, 1097-1100, 1995.

E. Atlas, and F. Flocke, Atmospheric Chemistry Division, National Center for Atmospheric Research, Boulder, CO 80303. (atlas@acd.ucar.edu; ffl@acd.ucar.edu)

M. A. Avery, and S. A. Vay, NASA Langley Research Center, Atmospheric Sciences Division, Hampton, VA, 23681. (s.a.vay@larc.nasa.gov; m.a.avery@larc.nasa.gov)

D. R. Blake, N. J. Blake, J. J. Colman, N. A. C. Johnston, A. S. Katzenstein, J. P. Lopez, S. Meinardi, F. S. Rowland, I. J. Simpson, and A. L. Swanson, University of California, Irvine, Department of Chemistry, Irvine, CA 92697-2025. (drblake@uci.edu; nblake@uci.edu; jonah@kokopelli.lanl.gov; akatzens@uci.edu; jplopez@uci.edu; smeinard@uci.edu; rowland@uci.edu; isimpson@uci.edu; aswanson@ea.oac.uci.edu)

B. C. Sive, Department of Chemistry, Central Michigan University, Mt. Pleasant, MI 48859. (Barkley.C.Sive@cmich.edu)